PACS numbers: 42.55.Lt; 34.50.Gb; 52.40.Mj
DOI: 10.1070/QE2010v040n02ABEH014226

Quenching of the resonance $5s(^3P_1)$ state of the krypton atom in collisions with krypton and argon atoms

D.A. Zayarnyi, A.Yu. L'dov, I.V. Kholin

***Abstract*. The processes of collision quenching of the resonance $5s[3/2]_1^o$ ($^3P_1$) state of the krypton atom are studied by the absorption probe method in electron-beam-excited high-pressure Ar – Kr mixtures with a low content of krypton. The rate constants of plasmochemical reactions $Kr^* + Kr + Ar \rightarrow Kr_2^* + Ar$ $[(4.40 \pm 0.44) \times 10^{-33}$ cm^6 s$^{-1}]$, $Kr^* + 2Ar \rightarrow ArKr^* + Ar$ $[(3.5 \pm 0.9) \times 10^{-36}$ cm^6 s$^{-1}]$, and $Kr^* + Ar \rightarrow$ products $+ Ar$ $[(3.84 \pm 0.38) \times 10^{-15}$ cm^3 s$^{-1}]$ are measured for the first time. The rate constants of similar reactions are refined for the metastable $5s[3/2]_2^o$ ($^3P_2$) state.**

Keywords: *inert gases, krypton, argon, plasmochemistry, quenching, absorption spectroscopy*.

1. Introduction

This paper continues the experimental investigation of the collision quenching processes of the excited 5s states of krypton atoms in the high-pressure Ar – Kr mixtures [1]. The quantitative data on such processes are virtually absent in the literature at present despite the fact that these processes play an important role both in the formation of the population inversion in high-pressure lasers on atomic transitions in inert gases [2], high-power krypton – fluorine lasers [3], krypton dimer lasers [4] and in other important applications related to the development of high-power compact excimer UV sources [5] and plasma display panels [6].

The aim of this paper is to measure the rate constants of collision quenching of Kr atoms at two lowest excited states – the resonance $5s[3/2]_1^o$ ($^3P_1$) and metastable $5s[3/2]_2^o$ ($^3P_2$) states (Fig. 1) – in dense mixtures of Kr with the buffer gas Ar. We studied practically important high-pressure Ar – Kr mixtures with low relative concentrations of Kr excited by a fast electron beam.

At high pressures, the resonance level of the Kr atom can be also considered metastable due to the radiation trapping effect. Under these conditions, the levels under study are quenched in the following three- and two-particle collision reactions:

D.A. Zayarnyi, A.Yu. L'dov, I.V. Kholin P.N. Lebedev Physics Institute, Russian Academy of Sciences, Leninsky prosp. 53, 119991 Moscow, Russia; e-mail: kholin@sci.lebedev.ru

Received 14 October 2009
Kvantovaya Elektronika **40** (2) 144 – 148 (2010)
Translated by I.A. Ulitkin

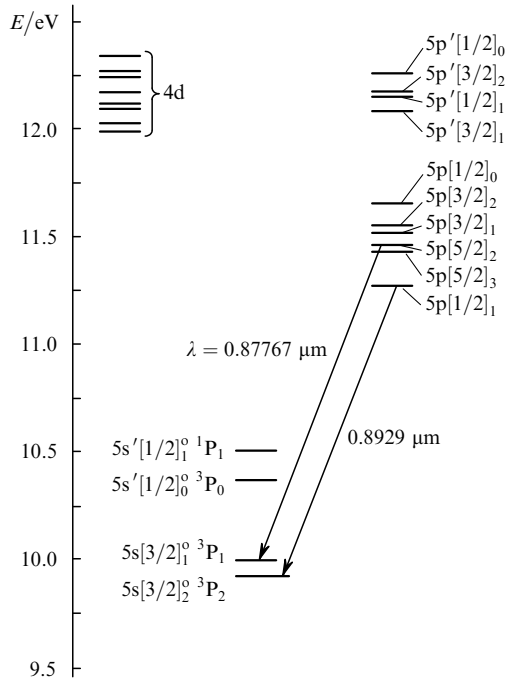

Figure 1. Energy level diagram of a krypton atom.

$$Kr^* + Kr + Ar \rightarrow Kr_2^* + Ar, \quad (1)$$

$$Kr^* + 2Ar \rightarrow ArKr^* + Ar, \quad (2)$$

$$Kr^* + Ar \rightarrow \text{products} + Ar. \quad (3)$$

In determining the rate constants of reaction (3), one should keep in mind that the experimentally obtained value is an upper estimate because it is needed to take into account the collision reactions of the excited krypton with atoms and impurity molecules M in the gas mixture under study (mainly in Ar):

$$Kr^* + M \rightarrow \text{products}. \quad (4)$$

The relative concentrations m of different impurities in purified Ar are not high (see below); however, due to large cross sections, the contribution of such reactions can be significant.

The rate constants of the reactions were measured with the absorption probe method [7, 8] by the dependences of the decay time of the studied states on the pressure and the

concentration ratio of the components of the working and buffer gases. For this purpose, we investigated in the afterglow of the gas mixture excited by a high-power fast electron beam the absorption dynamics of light pulses transmitted through the object under study at wavelengths 0.8929 and 0.87767 μm, corresponding to the optical transitions with a relatively large oscillator strength between the studied 5s levels of Kr and higher lying 5p levels (Table 1 and Fig. 1).

Table 1. Transitions under study in the Kr atom.

Transition	$\lambda/\mu m$
$5p[5/2]_2 - 5s[3/2]_1^o$	0.87767
$5p[1/2]_1 - 5s[3/2]_2^o$	0.8929

The main goal of the research in this paper is to measure the rate constants of the collision quenching of the resonance $5s[3/2]_1^o$ level (Table 2) in the reactions

$$Kr\left(5s[3/2]_1^o\right) + Kr + Ar \rightarrow Kr_2^* + Ar, \quad (5)$$

$$Kr\left(5s[3/2]_1^o\right) + 2Ar \rightarrow ArKr^* + Ar, \quad (6)$$

$$Kr\left(5s[3/2]_1^o\right) + Ar \rightarrow Kr\left(5s[3/2]_2^o\right) + Ar, \quad (7)$$

the data about which are absent in the literature. In addition, due to the improvement in the statistics, we refined the previously measured rate constants [1] of the reactions

$$Kr\left(5s[3/2]_2^o\right) + Kr + Ar \rightarrow Kr_2^* + Ar, \quad (8)$$

$$Kr\left(5s[3/2]_2^o\right) + 2Ar \rightarrow ArKr^* + Ar, \quad (9)$$

$$Kr\left(5s[3/2]_2^o\right) + Ar \rightarrow \text{products} + Ar \quad (10)$$

for the metastable $5s[3/2]_2^o$ level.

Table 2. Rate constants of the collision quenching of the $5s[3/2]_1^o$ and $5s[3/2]_2^o$ states of the Kr atom in the Ar–Kr mixture.

Reaction	Rate constants	References
(5)	$(4.40 \pm 0.44) \times 10^{-33}$ cm^6/s	Present paper
(6)	$(3.5 \pm 0.9) \times 10^{-36}$ cm^6/s	Present paper
(7)	$(3.84 \pm 0.38) \times 10^{-15}$ cm^3/s	Present paper
(8)	$(4.10 \pm 0.25) \times 10^{-33}$ cm^6/s	[1]
	$(3.56 \pm 0.36) \times 10^{-33}$ cm^6/s	Present paper
(9)	$(1.0 \pm 0.04) \times 10^{-33}$ cm^6/s	[12]
	$< 10^{-35}$ cm^6/s	[1]
	$(5.9 \pm 0.8) \times 10^{-36}$ cm^6/s	Present paper
(10)	$(0.69 \pm 0.06) \times 10^{-15}$ cm^3/s	[12]
	$(1.1 \pm 0.1) \times 10^{-15}$ cm^3/s	[13]
	$(3.78 \pm 0.23) \times 10^{-15}$ cm^3/s	[1]
	$(3.26 \pm 0.33) \times 10^{-15}$ cm^3/s	Present paper

2. Experimental setup

The experiments were performed using a Tandem pulsed laser setup with a cold-cathode electron gun [1, 2, 7, 8]. A 250-keV pulsed electron beam with a cross section 5×100 cm with a bell-shaped current envelope of duration ~ 2.5 μs at the base was introduced into a measurement chamber perpendicular to its optical axis through a 20-μm-thick titanium foil. The electron current density was 1.5 A cm^{-2}. The measurement chamber with the 5-L active volume was made of stainless steel. Before filling with gases under study, the chamber was pumped out down to the residual pressure of $\sim 10^{-5}$ Torr through a nitrogen trap; the leakage to the chamber did not exceed 10^{-3} Torr h^{-1}. We studied the mixture of the 99.98 % pure argon with the 99.9992 % pure krypton having the component ratio Ar:Kr = 200:1, 100:1, and 50:1 at a pressure of 1.75–4.0 atm.

The optical measurement scheme is shown in Fig. 2. ISI-1 broadband light source (*1*) with a pulse duration of ~ 30 μs [Fig. 3, curve (*1*)] served as a probe radiation source. At the output from the source, radiation was collimated into a beam with a diameter 5 cm, and after propagating through measurement chamber (*5*) with the mixture under study, it was collected to the entrance slit of MDR-2 high-transmission monochromator with a 600-lines mm^{-1} diffraction grating serving as a dispersion element. Radiation transmitted through the monochromator tuned to the studied wavelength λ was focused onto photoreceiver (*10*) consisting of a BPW34 fast pin photodiode (Infinition) and an AD8055 broadband operational amplifier (Analog Devices) placed in a metal housing with double screening. To suppress short-wavelength radiation in the diffraction second order in the probe radiation flux from the ISI-1 light source, we used KS-10 light filter (*10*).

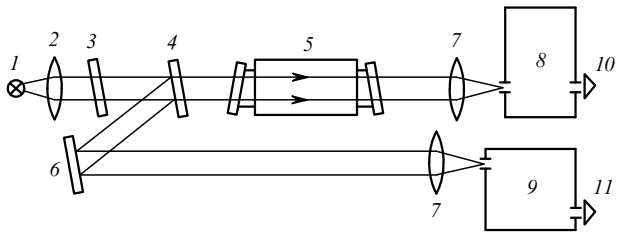

Figure 2. Optical scheme of the absorption measurements: (*1*) ISI-1 pulsed light source; (*2*) collimating lens; (*3*) KS-10 light filter; (*4*) beamsplitter; (*5*) measurement chamber; (*6*) folding mirror; (*7*) focusing lens; (*8*) MDR-2 high-transmission monochromator; (*9*) DMR-4 monochromator; (*10*, *11*) photodetectors.

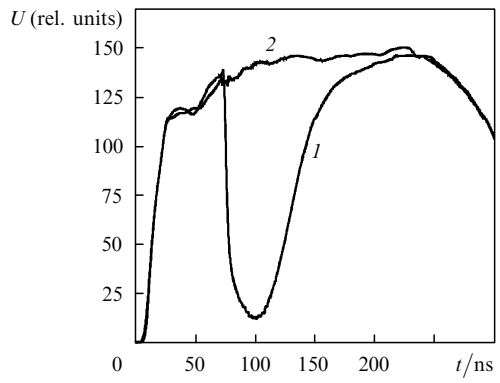

Figure 3. Time dependences of the signal from ISI-1 at $\lambda = 0.87767$ μm (for the $5s[3/2]_1^o$) propagated through the excited volume (*1*) and past it (*2*). The mixture is Ar:Kr = 100:1 at a pressure of 3.0 atm.

A part of radiation reflected from plane-parallel glass plate (*4*) placed in front of the measurement chamber was directed, past the measurement chamber, to DMR-4 monochromator (*9*) and second photodetector (*11*). Signals from the photodetectors were measured with a DSO-2010 two-channel digital oscilloscope (Link Instruments) connected to a computer.

Thus, the measurement scheme allowed us to detect simultaneously the shape and amplitude of the transmission pulse before and after the absorbing medium with a time resolution no worse than 100 ns.

3. Experiment

Excitation of the Ar–Kr mixtures under study by a fast electron beam leads to ionisation and excitation of atoms (mainly the buffer gas Ar). At high pressures in the chains of plasmochemical reactions of types

$$\mathrm{Ar}^+ + 2\mathrm{Ar} \rightarrow \mathrm{Ar}_2^+ + \mathrm{Ar}, \tag{11}$$

$$\mathrm{Ar}_2^+ + \mathrm{Kr} \rightarrow \mathrm{Kr}^+ + 2\mathrm{Ar}, \tag{12}$$

$$\mathrm{Kr}^+ + \mathrm{Kr} + \mathrm{Ar} \rightarrow \mathrm{Kr}_2^+ + \mathrm{Ar} \tag{13}$$

there occurs a transition of excitation to molecular krypton ions. Dissociation recombination of these ions with the electrons,

$$\mathrm{Kr}_2^+ + \mathrm{e} \rightarrow \mathrm{Kr}^{**} + \mathrm{Kr}, \tag{14}$$

leads to the production of krypton atoms in different highly excited states, which then rapidly relax (due to collisions with heavy particles and secondary electrons as well as the radiation decay) into lower excited 5s states of the Kr atom.

In the electron beam afterglow after the end of the recombination and relaxation processes, the concentration of the states studied in this paper should be determined mainly by the processes of their decay in reactions (1)–(4):

$$\frac{\mathrm{d}[\mathrm{Kr}^*]}{\mathrm{d}t} = -k_1[\mathrm{Kr}][\mathrm{Ar}][\mathrm{Kr}^*] - k_2[\mathrm{Ar}]^2[\mathrm{Kr}^*] - (k_3 + k_4 m)[\mathrm{Ar}][\mathrm{Kr}^*], \tag{15}$$

where k_1 and k_2 are the rate constants of excimerisation in reactions (1) and (2), respectively; k_3 is the rate constant of two-particle relaxation (3); k_4 is the quenching rate constant by impurities in reaction (4).

In this case, the time dependence of the populations of the excited Kr^* state can be represented as an exponential dependence

$$[\mathrm{Kr}^*](t) = N_0 \exp(-t/\tau_\mathrm{d}) \tag{16}$$

with the decay rate

$$\tau_\mathrm{d}^{-1} = k_1[\mathrm{Kr}][\mathrm{Ar}] + k_2[\mathrm{Ar}]^2 + (k_3 + k_4 m)[\mathrm{Ar}]. \tag{17}$$

When monochromatic radiation at the wavelength of the transition from the highly excited state to the state under study propagates through the excited medium, the linear absorption coefficient k should be proportional to the concentration of the atoms in this state:

$$k(t) \sim [\mathrm{Kr}^*](t). \tag{18}$$

In our case, for the dimensions of the input and output slits of the MDR-2 monochromator (~ 0.2 mm), providing a satisfactory signal-to-noise ratio in the measurement channel, the width of the monochromator instrument function in the pressure range from 1.75 to 40 atm significantly exceeds the linewidth of the observed optical transition. In this situation, the Beer–Lambert–Bouguer law, generally speaking, is not fulfilled and it is necessary to use its empirical or the so-called modified form [9, 10] binding the measured transmission coefficient T with the absorption coefficient T by the relation

$$\ln(1/T) = (kL)^\gamma. \tag{19}$$

Here, L is the length of the electron-beam-excited absorbing medium, while γ is a dimensionless factor depending on the ratio of the absorption linewidths and the monochromator instrument function. Investigation [1] of the experimental dependences

$$\ln\ln(1/T) = \mathrm{const} - \gamma \ln L \tag{20}$$

pointed out to the applicability of the Beer–Lambert–Bouguer law under our conditions and made it possible to estimate, in this series of the experiments, the dimensional factor γ as 0.5 (see details in [11]).

Thus, it follows from expression (19) taking into account relation (18) and time dependence $[\mathrm{Kr}^*](t)$ expected according to (16) that the trailing edge of the absorption pulse should be of a purely exponential character:

$$\ln[1/T(t)] \sim \exp(-\gamma t/\tau_\mathrm{d}). \tag{21}$$

Taking the logarithm of expression (21) leads to the following linear expression for the time dependences of the transmission coefficient T at the trailing edge:

$$\ln\ln[1/T(t)] = \mathrm{const} - \gamma t/\tau_\mathrm{d}. \tag{22}$$

In practice, the situation is somewhat more complicated [1].

Figure 3 presents the typical oscillograms of the probe radiation pulse from the ISI-1 source obtained for the resonance level at the wavelength of the $5\mathrm{p}[5/2]_2 - 5\mathrm{s}[3/2]_1^\mathrm{o}$ transition. The comparison of the signal amplitudes at the input [curve (*2*)] and output [curve (*1*)] of the excited active medium makes it possible to determine the transmission coefficient T of this medium at the wavelength to which the monochromator is tuned. Figure 4 illustrates, for the oscillograms of Fig. 3, the time dependences of the absorption and the quantity $\ln\ln(1/T)$ for the trailing edge of this pulse.

As we noted in our previous paper [1], due to large characteristic times τ_d of the collision quenching processes in the studied levels $\mathrm{Kr}^*(6\mathrm{s})$, it is necessary to take into account the influence of even weak recombination fluxes continuing to populate these levels even in the afterglow upon completion of the electron pump pulse on their populations. In the experiment, the influence of the recombination effect is manifested in a slight difference from the exponential time dependence of the trailing edge of the absorption pulse in Fig. 4a and, therefore, in the nonlinear

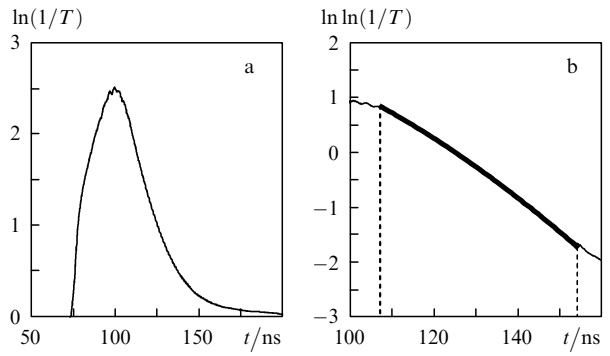

Figure 4. Time dependences of absorption (a) and quantity $\ln\ln(1/T)$ approximated by the second-order curve (heavy curve) (b) for the signals from Fig. 3.

character of the time dependence of the quantity $\ln\ln(1/T)$ (Fig. 4b), which differs from (22).

To calculate the exponential component of the trailing edge of the absorption pulse, we processed numerically the obtained time dependences by approximating the curves in Fig. 4b by a quadratic polynomial:

$$\ln\ln(1/T) = p - g^2(t - t_0)^2 - k_d(t - t_0) \tag{23}$$

(p, g, k_d are the approximation parameters), in which its linear part determines the searched-for rate of the collision quenching of the studied level $k_d = \gamma/\tau_d$, and the small quadratic correction – its population dynamics.

The quenching rates were calculated by the experimental dependences (23) using the method of least squares upon varying the coefficients p, k_d, and t_0 with the use of the Levenberg–Marquardt algorithm. In this case, the best result was obtained at the ratio of the rate coefficients $g = 0.6k_d$. We calculated a set of the experimental data for the mixtures with the component ration Ar:Kr = 50:1, 100:1, and 200:1 at a pressure 2.0–4.0 atm for the $5s[3/2]_1^o$ level and at a pressure of 1.75–4.0 atm for the $5s[3/2]_2^o$ level with a step 0.25 atm.

In the coordinates of Fig. 4a, to function (23) there corresponds the function

$$\ln(1/T) = (\exp p)\exp\left[-g^2(t - t_0)^2\right] \times \exp[-k_d(t - t_0)], \tag{24}$$

representing a superposition of the exponential function describing the collision quenching processes, and the Gaussian preexponential giving a correction to the recombination and relaxation processes. Determination of the real shape of the preexponential curve in the analytic form is hardly possible due to the variety and complexity of the reactions depending, in particular, on the time-changing temperature and density of secondary electrons. However, in practice, this 'mnemonic' description of the dynamic range of variations in the transmission coefficient $T = 0.1$–0.9 (see Fig. 3) yields rather satisfactory results. Thus, Fig. 5 presents for each Ar–Kr mixture the dependences of the quantity $k_d[Ar]^{-1}$ on the buffer gas concentration. In this case, as provided by the linear character [expected according to (17)] of the dependences:

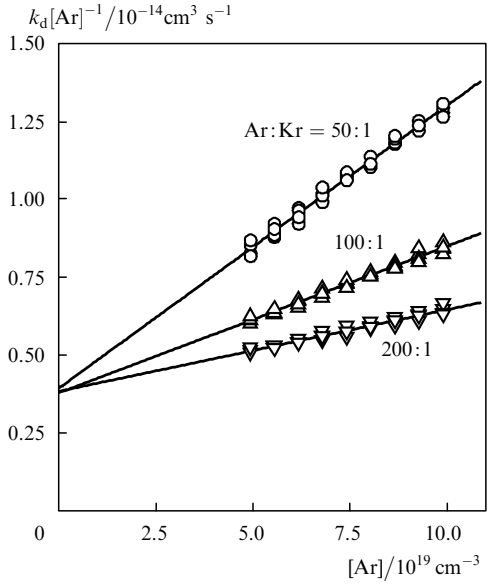

Figure 5. Dependences of the reduced quenching rates $k_d[Ar]^{-1}$ of the $5s[3/2]_1^o$ level on the argon concentration in different Ar–Kr mixtures.

$$k_d[Ar]^{-1} = (\delta k_1 + k_2)[Ar] + (k_3 + k_4 m) \tag{25}$$

($\delta = [Kr]/[Ar]$), the experimental points indeed lie with a good accuracy on the straight lines originating from the ordinate axis, which indicates the adequacy of representation (24) and correctness of the whole procedure of the experimental data processing.

The set of experimental values $k_d^{(i)}([Kr], [Ar])$ obtained by the above method was used to determine the rate constants of plasmochemical reactions (1), (2), and upper estimates with the accuracy to the unknown value $k_4 m$ of reaction rate (3). The rate constants k_1, k_2, and k_3 presented in Table 2 were calculated by using the Levenberg–Marquardt algorithm upon varying the searched-for constants in the relations

$$k_d^{(i)} = k_1[Kr]_i[Ar]_i + k_2[Ar]_i^2 + k_3[Ar]_i \tag{26}$$

simultaneously for the entire set of the experimental values $k_d^{(i)}$. The essence of the procedure consisted in constructing a curvilinear surface in the coordinates [Kr], [Ar]

$$S([Kr], [Ar]) = k_1[Kr][Ar] + k_2[Ar]^2 + k_3[Ar], \tag{27}$$

which deviates, in terms of this method, from the set of the experimental points.

The obtained data confirm the conclusion of paper [1] about the fact that under our experimental conditions, the collision quenching of the 5s state of the Kr atom in the Ar–Kr mixture occurs during the three-particle reactions accompanied by the formation of a homonuclear dimer Kr_2^* (1) and during two-particle reactions (3), (4). At the same time, three-particle reaction (2) accompanied by the formation of a heteronuclear dimer $ArKr^*$ virtually does not participate in the collision quenching of Kr^*. The latter circumstance can be explained by the fact that the heteronuclear dimer obtained in reaction (2) proves unstable due to the low binding energy [14] and is actively decomposed

into the initial components in inverse collision reactions. In this case, the measured effective rate constant of the $ArKr^*$ dimer formation is close to zero.

4. Conclusions

We have studied for the first time the quenching of the resonance $Kr^*(5s[3/2]_1^o)$ state in the mixtures close in their composition and pressure to those used in excimer lasers and high-pressure lasers on atomic transitions of inert gases. We have shown that the main relaxation channels for this state are the excimerisation processes accompanied by the formation of the dimer Kr_2^* with the rate constant 4.40×10^{-33} cm^6 s^{-1} and quenching by the buffer gas with the rate constant 3.84×10^{-15} cm^3 s^{-1}. At the same time, reactions accompanied by the formation of heteronuclear dimers virtually do not play any role.

Due to the improvement in the statistics, we have refined the rate constants of similar reactions for the metastable $Kr^*(5s[3/2]_2^o)$ state, which, as was expected, correspond, within the measurement accuracy, to the values we obtained for the first time in paper [1].

Acknowledgements. The authors thank N.N. Ustinovskii for his collobaration and useful discussions.

References

1. Zayarnyi D.A., L'dov A.Yu., Kholin I.V. *Kvantovaya Elektron.*, **39** (9), 821 (2009) [*Quantum Electron.*, **39** (9), 821 (2009)].
2. Kholin I.V. *Kvantovaya Elektron.*, **33** (2), 129 (2003) [*Quantum Electron.*, **33** (2), 129 (2003)].
3. Zvorykin V.D., Arlantsev S.V., Bakaev V.G., Gaynutdinov R.V., Levchenko A.O., Molchanov A.G., Sagitov S.I., Sergeev A.P., Sergeev P.B., Stavrovskii D.B., Ustinovskii N.N., Zayarnyi D.A. *J. Phys. IV*, **133**, 567 (2006).
4. Zvereva G.N., Lomaev M.I., Rybka D.V., Tarasenko V.F. *Opt. Spektros.*, **102** (1), 36 (2007).
5. Robert E., Sarroukh H., Cachoncinlle C., Viladrosa R., Hochet V., Eddaoui S., Pouvesle J.M. *Pure Appl. Chem.*, **77** (2), 463 (2005).
6. Tae-Won Kim, Soon-Up Kwon, Ho-Jung Hwang. *J. Korean Phys. Soc.*, **42**, S848 (2003).
7. Zayarnyi D.A., Kholin I.V. *Kvantovaya Elektron.*, **33** (6), 474 (2003) [*Quantum Electron.*, **33** (4), 474 (2003)].
8. Semenova L.V., Ustinovskii N.N., Kholin I.V. *Kvantovaya Elektron.*, **34** (3), 189 (2004) [*Quantum Electron.*, **34** (3), 189 (2004)].
9. Oka T. *Res. Rep. Nagaoka Tech. Coll.*, **13** (4), 207 (1977).
10. Davis C.C., McFarlane R.A. *J. Quant. Spectrosc. Rad. Transfer*, **18**, 151 (1977).
11. Zayarnyi D.A., Kholin I.V., Chugunov A.Yu. *Kvantovaya Elektron.*, **22** (3), 233 (1995) [*Quantum Electron.*, **25** (3), 217 (1995)].
12. Kolts J.H., Setser D.W. *J. Chem. Phys.*, **68** (11), 4848 (1978).
13. Sobczynski R., Setser D.W. *J. Chem. Phys.*, **95** (5), 3310 (1991).
14. Nowak G., Fricke J. *J. Phys. B: At. Mol. Phys.*, **18**, 1355 (1985).